UDC 550.384 + 551.24

Semyon CHERKES

[1] Institute of Geophysics, National Academy of Sciences of Ukraine, Akademika Palladina Ave. 32, Kyiv, 03142, Ukraine, tel. +38(050)1565912, e-mail SemyonCherkes@gmail.com

https://doi.org/10.23939/jgd2025.02.129

NEW RESULTS OF PALAEOMAGNETIC AND ROCK MAGNETIC STUDIES OF GABBROIDS OF THE KOROSTEN PLUTON OF THE UKRAINIAN SHIELD

Palaeomagnetic and rock magnetic studies were conducted on anorthosites and gabbros from the Volodarsk-Volynskyi massif of the Korosten pluton to obtain new palaeomagnetic determinations that meet modern reliability criteria. The results confirm that the main magnetic carriers in these rocks are magnetite and titanomagnetite, which contain a small amount of Ti. A bipolar characteristic component of magnetisation, isolated in the temperature range of 500–580 °C, demonstrates a primary origin and thermoremanent nature. The new 1.76 Ga palaeomagnetic pole (Φ = 29.3°, Λ = 168.2°, A_{95} = 3.3°, N = 6) is in good agreement with palaeomagnetic determinations of similar age for the Inhul and Volyn domains of the Ukrainian Shield. This suggests that the evolution of these domains within the unified structure of the Ukrainian Shield began at least 1.76 Ga. To clarify the timing of the amalgamation of the East European Platform, and to calculate its palaeolatitudinal position and kinematic parameters (latitudinal drift and angular rotation velocity) of its segments, a selection of the most reliable Palaeoproterozoic palaeomagnetic determinations for Fennoscandia and Sarmatia was compiled. Palaeogeographic reconstructions of these segments were performed for specific time intervals. According to the palaeomagnetic data, their final amalgamation occurred no earlier than 1.76 Ga. At that time, these segments were located in the equatorial zone, and the Ukrainian Shield (as part of Sarmatia) was rotated ~40° counterclockwise relative to Fennoscandia.

Keywords: Korosten pluton; Ukrainian Shield; gabbroids; palaeomagnetism; rock magnetism; palaeomagnetic pole; palaeogeographic reconstructions.

Introduction

The East European Platform (Baltica palaeo-continent) is a key element in palaeogeographic and palaeotectonic reconstructions of the Precambrian. This importance arises from its detailed geological and geophysical investigation as well as the presence of reliably dated and accessible geological formations of various ages. The East European Platform (EEP) comprises distinct segments–Fennoscandia, Sarmatia, and Volgo-Uralia–each with its own evolutionary history [Bogdanova et al., 2005]. It is essential to determine the drift characteristics of these segments and establish quantitative constraints on the timing of their consolidation. This issue can be addressed through palaeomagnetic studies, particularly those of Palaeoproterozoic rocks from the Ukrainian Shield, supported by geochronological and geological data.

Palaeomagnetic data enable the modelling of tectonic block movement and the estimation of the geometry and mechanisms of geomagnetic field generation. The availability of dated palaeomagnetic datasets for individual tectonic blocks enables the determination of their palaeolatitude and orientation in ancient geological times. A sequential set of such determinations (the apparent polar wander path, APWP) allows estimation of the rates of latitudinal drift and angular rotation of individual tectonic units. However, the existing palaeomagnetic datasets for the EEP are irregular in both age coverage and reliability, with a particularly notable scarcity for the Precambrian, owing to the limited number of formations suitable for palaeomagnetic investigation.

Current state of the problem

Over the past decades, both the equipment and techniques used in palaeomagnetic studies have improved significantly, leading to a substantial increase in the quantity and quality of palaeomagnetic data. To facilitate the selection and summarisation of such data, global palaeomagnetic databases have been established [Veikkolainen et al., 2017; Jarboe et al., 2012; Pisarevsky, 2005] and are regularly updated. Currently, there are approximately 8,000 determinations for the Phanerozoic and about 3,500 for the Precambrian (~200 corresponding to the Archean, ~400 to the Palaeoproterozoic, ~2,000 to the Mesoproterozoic, and ~900 to the Neoproterozoic).

For the Precambrian of the EEP, a considerable number of determinations (~940) have been obtained from rocks of the Baltic Shield (Fennoscandia), while significantly fewer (~100 and ~70) have been derived from rocks of the Eastern Urals (Volgo-Uralia) and the Ukrainian Shield (Sarmatia), respectively [Veikkolainen et al., 2017]. However, the number of determinations meeting the Van der Voo reliability criteria ($Q \geq 3$) [Van der Voo, 1990] – considered the lower threshold for reliable palaeogeographic reconstructions–is only ~430 for the entire Precambrian and ~175 for the Palaeoproterozoic of the EEP. Furthermore, palaeomagnetic data are lacking for certain time intervals across various parts of the EEP, including the entire Palaeoproterozoic of the Volgo-Uralia.

Reconstructions based on quantitative palaeomagnetic data obtained from Precambrian rocks of the Ukrainian Shield, which meet modern reliability criteria [Buchan, 2013], are limited and often ambiguous. This is due to several factors. Firstly, the specific characteristics of these formations impose a number of constraints on the application of the p-alaeomagnetic method, including challenges associated with performing field tests of palaeomagnetic stability. In addition, the criteria used for selecting palaeomagnetically stable rocks (as well as those for assessing the reliability of the obtained data) were developed primarily for the Phanerozoic [Van der Voo, 1990] and are often not fully applicable to Precambrian rocks. Secondly, the reliability and precision of geochronological determinations for the Precambrian are crucial for the correct interpretation of palaeomagnetic data. Thirdly, the distribution of palaeomagnetic determinations is uneven in both age and geographic coverage, reflecting the irregular availability of suitable formations for study.

Some of the most promising Palaeoproterozoic formations for palaeomagnetic studies within the Ukrainian Shield are the Korosten and Korsun-Novomyrhorod anorthosite–rapakivi granite complexes. Modern geochronological determinations are available for the rocks of these complexes [Shumlyanskyy et al., 2017]. Previous palaeomagnetic studies have identified the most informative rock varieties for investigation [Mikhailova et al., 1994; Elming et al., 2001; Bakhmutov et al., 2018; Bakhmutov et al., 2023; Cherkes et al., 2023a].

The present **study aims** to obtain new, reliable palaeomagnetic determinations for the basic rocks of the Volodarsk-Volynskyi massif of the Korosten pluton and to calculate the kinematic parameters of the EEP and its segments in the Palaeoproterozoic, based on a selection of the most reliable palaeomagnetic data.

Geology of the Korosten pluton

The Korosten plutonic complex is one of the most typical and well-studied examples of Palaeoproterozoic anorthosite–rapakivi granite complexes in both Ukraine and the world. It comprises the Korosten pluton (KP) itself, along with several smaller intrusive bodies, metasomatic formations, and contact-metamorphic rocks distributed within the KP framework. Intrusions of the Korosten complex are emplaced into the folded Palaeoproterozoic basement of the north-eastern part of the Volyn domain of the Ukrainian Shield, near its boundary with the Ros-Tikych domain (Fig. 1, *a*).

The KP has an approximately isometric shape, covers an area of about 10,000 km^2, and extends 100 km in the meridional direction and 150 km from west to east. Its petrographic composition includes both basic and acidic rocks, with intermediate varieties being relatively rare. The basic rocks are represented by gabbro–anorthosite massifs, the largest of which are Volodarsk-Volynskyi, Chopovychi, and Fedorivka. The acidic rocks correspond to granitoid massifs, among which Narodychi, Malyn, Chervonoarmiysk, and Sydorovychi are the most prominent. Rapakivi and rapakivi-like granites are the predominant rock types, covering about 75 % of the pluton area. anorthosites, gabbro–anorthosites, and gabbros account for approximately 23 %, while hybrid rocks account for no more than 2 % [Mytrokhyn et al., 2011].

According to zircon and baddeleyite U–Pb dating, the age of the Korosten complex rocks ranges from 1815 Ma to 1743 Ma, with two major stages of magmatic activity occurring at intervals of 1800–1780 Ma and 1768–1755 Ma [Shumlyanskyy et al., 2017]. During these stages, granitoid and basic magmatism alternated [Mytrokhyn, 2011]. Based on previous studies [Mytrokhyn, 2011; Shumlyanskyy, 2012; Shumlyanskyy et al., 2017], five age series have been identified for the basic rocks of the KP: A_1 – early anorthositic (1800–1780 Ma); A_2 – main anorthositic (1761–1758 Ma); G_3 – early gabbroic; G_4 – late gabbroic (1763–1757 Ma); and D_5 – dyke series, which formed throughout the entire period of KP formation. The Volodarsk-Volynskyi Massif (VVM) is a polyphase intrusion composed of rock associations of different ages, related to the main anorthosite series (A_2) and the gabbroic series $G_{3–4}$. It is the largest gabbro–anorthosite massif both within the KP and within the EEP [Mytrokhyn, 2011].

The VVM is located in the south-western part of the KP and covers an area of approximately 1,250 km^2. It is surrounded by granitoids of the Korosten complex (Fig. 1, *b*). In the north-eastern part, the VVM borders the rocks of the Chopovychi Massif, and in the south, it adjoins the metamorphic formations of the Teteriv Series and, locally, the granitoids of the Zhytomyr Complex [Shumlyanskyy et al., 2017].

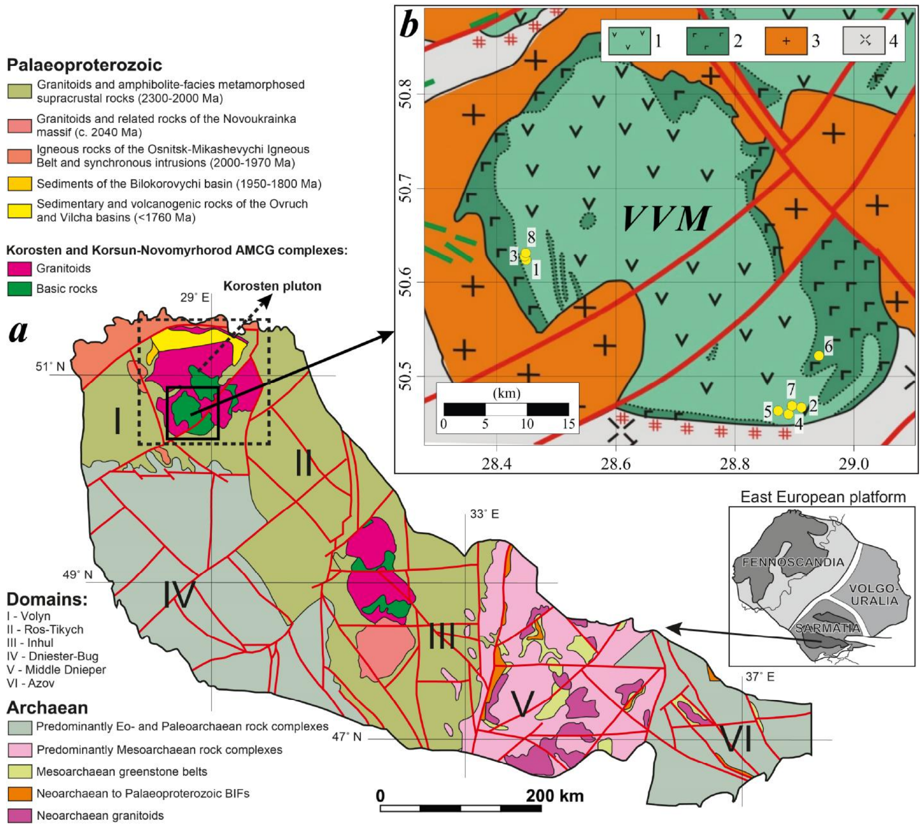

Fig. 1. Schematic geological map of the Ukrainian Shield (a) and the Volodarsk-Volynskyi massif of the Korosten pluton with sampling sites (b). Adapted from [Shumlyanskyy et al., 2017; Mytrokhyn, 2011].

Legend (a): see Fig. Legend (b): 1 – anorthosites and gabbro-anorthosites, 2 – gabbros, gabbro–norites, gabbro–monzonites and monzonites, 3 – rapakivi and rapakivi-like granites, 4 – host granites and migmatites; yellow circles show the sampling sites locations, corresponding numbers are the site indexes according to Table 1 and Fig. 2, *e*–*g* and 3.

Geological and geophysical data indicate that the VVM occurs as a subhorizontal plate up to 7 km thick, with boundary zones containing subvertical gabbroic dyke-like bodies that extend to depths of 7–10 km [Bogdanova et al., 2004]. These are interpreted as ring-shaped magma conduits [Mytrokhyn, 2011]. Hybrid rocks, such as gabbro–monzonites, monzonites, monzodiorites, and syenites, occur along the margins of the massif at the contact zones between gabbros and granitoids. A major part of the VVM was formed during the fourth intrusive phase, dated to 1761–1758 Ma [Shumlyanskyy et al., 2017], corresponding to the main anorthosite series (A_2). The massif is predominantly represented by coarse- to giant-grained anorthosites and gabbro–anorthosites transitioning into leucocratic gabbros.

Materials and methods

Palaeomagnetic and rock magnetics studies

Before sampling, particular attention was given to identifying the least weathered areas of rock outcrops, from which samples were collected. Sampling was performed using a portable rock drill based on a Stihl chainsaw and/or a Makita drill. Core samples, with a diameter of ~2.54 cm and a length of 7–10 cm, were oriented using a Pomeroy OR-2 device, which utilized both a Brunton magnetic compass and a solar compass. For subsequent measurements, 2–4 specimens were prepared from each core, each with a height of 2.2 cm and a diameter of 2.54 cm.

The research was conducted using equipment at the palaeomagnetic laboratory of the Centre for the Collective Use of Magnetometric Equipment, Institute of Geophysics, National Academy of Sciences of Ukraine. Stepwise thermal demagnetisation and measurements of natural remanent magnetisation (NRM) were performed in a magnetically shielded room, MMLFC (Magnetic Measurements, UK). Heating was carried out using an MMTD80 furnace (Magnetic Measurements) in temperature increments of 10–50 °C, up to 590–640 °C. Alternating field demagnetisation was conducted using an LDA-3A device (AGICO, Czech Republic) in fields up to 100 mT. NRM and magnetic susceptibility were measured with a JR-6A magnetometer (AGICO) and an MFK1-FB kappabridge (AGICO), respectively.

The NRM components were determined using principal component analysis [Kirschvink, 1980] and remagnetisation circle analysis [Halls, 1976], implemented in Remasoft 3.0 software [Chadima and Hrouda, 2006].

Thermomagnetic analysis was conducted to identify the magnetic carriers of the NRM. This analysis assessed the dependence of magnetic susceptibility on temperature, using a KLY-5A kappabridge equipped with a CS4 apparatus module from AGICO. To determine the unblocking temperature ranges of magnetic minerals with different coercivity spectra, the Lowrie test was conducted [Lowrie, 1990]. Samples were sequentially magnetized along three orthogonal axes in fields of 2.5 T, 0.4 T, and 0.12 T, respectively, followed by stepwise thermal demagnetisation. In addition, isothermal magnetisation curves were analyzed for fields up to 1.25 T.

Poles selection and palaeogeographic reconstruction

The selection of palaeomagnetic determinations for the EEP was carried out using the palaeomagnetic databases Global Paleomagnetic Data Base [Pisarevsky, 2005], Magnetics Information Consortium [Jarboe et al., 2012], and Precambrian Database PALEOMAGIA [Veikkolainen et al., 2017]. The selection process followed modern criteria for assessing the reliability of palaeomagnetic determinations [Van der Voo, 1990; Buchan, 2013]. The polarity of the poles was determined according to the principle of the shortest distance between chronologically nearest poles. Palaeogeographic reconstructions and calculations of the kinematic parameters of the EEP were performed using the GMAP2012 [Torsvik and Smethurst, 1999] and GPlates [Müller et al., 2018] software.

Results and discussion

Palaeomagnetic studies

According to studies of pilot collections of KP rocks [Bakhmutov et al., 2018; Bakhmutov et al., 2023; Cherkes et al., 2023a], the palaeomagnetically most informative rock varieties were identified as anorthosite and gabbro–anorthosite, while gabbro and monzonite were found to be less informative. These results are consistent with previous studies of KP rocks [Mikhailova et al., 1994; Elming et al., 2001].

Table 1

Site-mean palaeomagnetic directions and virtual geomagnetic poles

No.	Φ,°N	Λ, °E	Rock	T_{ub}, °C	*n/N*	*D*, °	*I*, °	*k*	α_{95} (MAD), °	Φ, °N	Λ, °E	*dp/dm* °
1	50.6236	28.4494	Gabbro-anorthosite	**470–570^{PCA}**	**18/16**	**212.3**	**6.4**	**40**	**5.9**	**29.5**	**170.7**	**3.0/5.9**
				200–540^{RC}	18/10	210.6	9.8	-	(2.4)			
2	50.4668	28.9117	Anorthosite	**470–590^{PCA}**	**25/12**	**35.1**	**2.5**	**12**	**13.4**	**32.5**	**165.9**	**6.7/13.4**
				440–580^{RC}	25/13	41.2	11.6	-	(9.3)			
3	50.6274	28.4469	Olivine gabbro	**480–620^{PCA}**	**35/20**	**214.1**	**7.3**	**94**	**3.4**	**28.4**	**169.0**	**1.7/3.4**
				200–600^{RC}	35/12	212.4	9.7	-	(3.3)			
4	50.4597	28.8901	Anorthosite	**490–580^{PCA}**	**48/14**	**36.3**	**1.1**	**8.5**	**14.5**	**31.4**	**165.0**	**7.3/14.5**
				150–580^{RC}	48/18	30.0	31.4	-	(7.3)			
5	50.4631	28.8724	Gabbro	360–560^{RC}	27/9	218.0	2.5	-	(14.6)			
6	50.5218	28.9411	Gabbro	**420–580^{PCA}**	**37/20**	**213.9**	**7.2**	**20**	**7.5**	**28.6**	**169.6**	**3.8/7.5**
				380–580^{RC}	37/20	211.6	4.5	-	(5.2)			
7	50.4686	28.8959	Anorthosite	470–580^{PCA}	17/16	203.6	29.8	12	11.1	20.4	184.7	6.8/12.3
				150–580^{RC}	17/10	201.9	23.5	-	(8.7)			
8	50.6310	28.4484	Olivine gabbro	**500–570^{PCA}**	**33/24**	**215.4**	**12.0**	**64**	**3.7**	**25.6**	**168.7**	**1.9/3.8**
				440–580^{RC}	33/7	209.0	13.4	-	(3.8)			

Note: No. is index of the sampling site according to Fig. 1 *b*, 2 *e–g* and 3; φ and λ are latitude and longitude of the sampling site, respectively; T_{ub} is unblocking temperature range of NRM; *n/N* is ratio of the total number of specimens studied to the number of specimens with identified ChRM used in calculations; *D* and *I* are site-mean declination and inclination of NRM directions, respectively; *k* is Fisher precision parameter of the site-mean direction; α_{95} (MAD) is radius of the confidence circle for the site-mean direction at 95% probability level (maximum angular deviation); Φ and Λ are latitude and longitude of the virtual geomagnetic pole; *dp/dm* is a semi-axes of the confidence ellipse for the virtual geomagnetic pole at a 95% probability level. The superscripts "PCA" and "RC" near the unblocking temperature indicate the component isolation method: principal component analysis or remagnetisation circles method, respectively. The high-temperature ChRM used to calculate the average palaeomagnetic direction and pole is shown in bold.

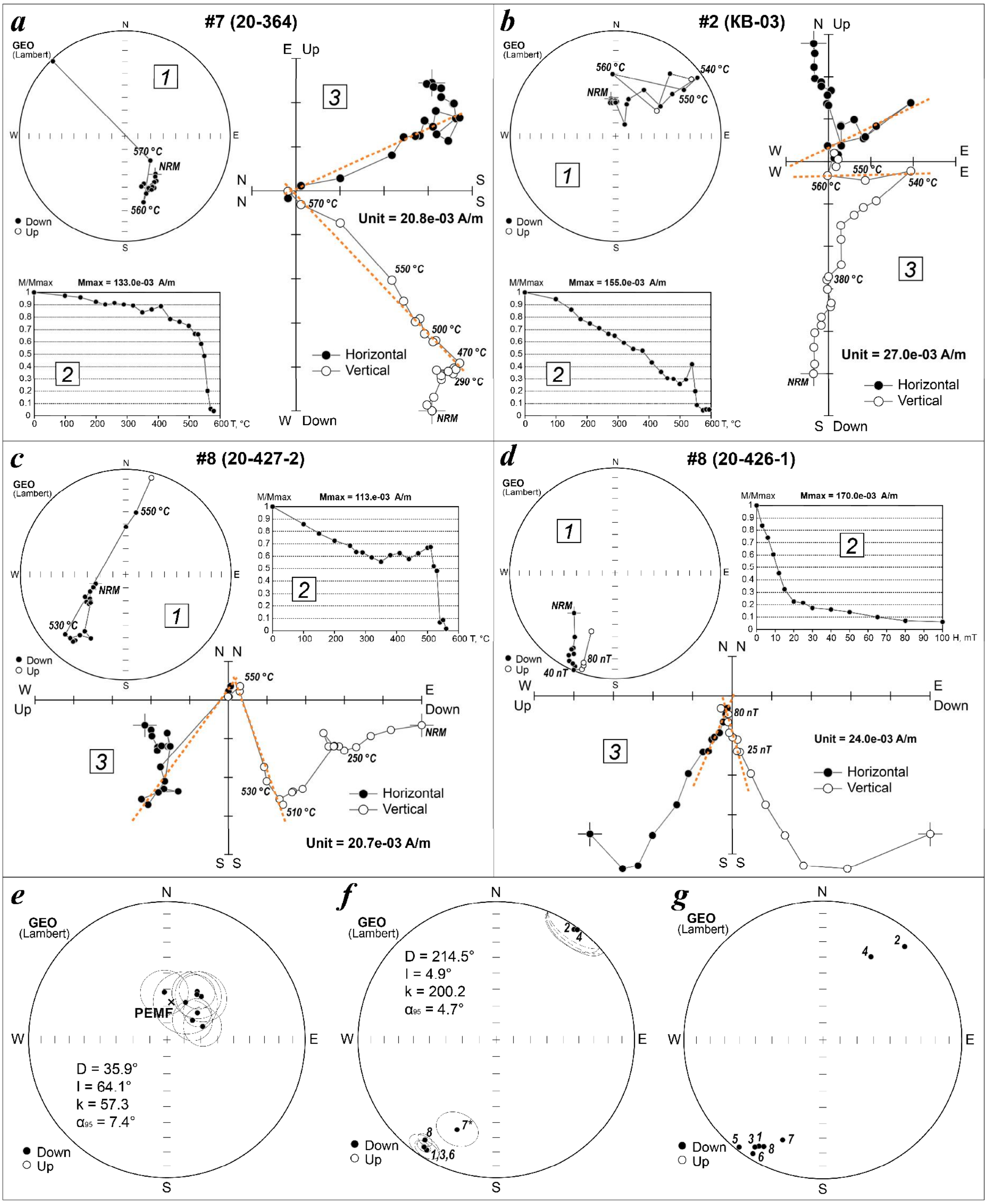

Fig. 2. Examples of demagnetisation of anorthosite (*a*, *b*) and gabbro (*c*, *d*) specimens, site-mean palaeomagnetic directions of the low-temperature component of remanent magnetisation (*e*) and the high-temperature characteristic component of remanent magnetisation (*f*), identified by principal component analysis, as well as directions identified using the remagnetisation circles method (*g*).

Legend (*a–d*): 1 – stereographic projections of NRM vectors during demagnetisation (filled and empty circles are projections in the lower and upper hemispheres, respectively); 2 – NRM value (M/Mmax) during demagnetisation; 3 – orthogonal diagrams of NRM vectors (Zijderveld diagrams) on horizontal and vertical planes; the orange line represents the identified ChRM vector. The numbers near the projections of the site-mean directions of the magnetisation (*e–g*) are the sampling site numbers according to Table 1 and Fig. 1, *b*. The cross (*e*) indicates the direction of the present Earth's magnetic field (PEMF) in the sampling area. The asterisk (*f*) indicates pole No. 7*, which was excluded from the calculations.

In this research, new collections of basic rock samples from the VVM were analyzed, representing eight sampling sites (see Fig. 1 *b*). The results are presented in Table 1 and Fig. 2. The NRM values of the studied samples vary across a relatively wide range and can differ significantly even within a single sampling site. In general, anorthosites exhibit higher NRM values (120×10^{-3} A/m to 400×10^{-3} A/m) compared with gabbros (80×10^{-3} A/m to 220×10^{-3} A/m), which corresponds to the typical NRM range for KP rocks [Bakhmutov et al., 2025]

Based on a comparison of demagnetisation results from the pilot specimen collection–using both alternating magnetic field (e. g., see Fig. 2, *d*) and thermal demagnetisation methods (see Fig. 2, *a–c*)–the latter technique was preferred.

Two magnetisation components were identified in most samples. The low-temperature component (LTC) is generally demagnetized at unblocking temperature (T_{ub}) range of 350–450 °C, and occasionally up to 540 °C. The contribution of this component to the NRM varies: in anorthosites, it averages 10–35 % (see Fig. 2, *a*), while in gabbros it is significantly higher, ranging from 30% to 60 % (see Fig. 2, *c*). The LTC is most likely associated with viscous magnetisation, as its direction is close to that of the present Earth's magnetic field (PEMF) at the sampling site. On average, however, for all collections, the LTC direction is slightly shifted eastward relative to the PEMF (see Fig. 2, *e*). The mean direction of the viscous LTC is characterized by the following statistical parameters: D = 35.9°, I = 64.1°, k = 57.3, α_{95} = 7.4°, N = 8.

The high-temperature characteristic remanent magnetisation (ChRM) component accounts for up to 90 % of the initial NRM in anorthosites (see Fig. 2, *a*) and approximately 50% in gabbros (see Fig. 2, *c*). In some anorthosites, however, the viscous component is dominant (see Fig. 2, *b*). For most specimens, the ChRM is defined by linear segments of orthogonal projections within the 500–580 °C T_{ub} range, based on 4–6 data points (see Fig. 2 *a*, *c*), although in some cases it extends over a broader interval (360–620 °C). The ChRM vector in general trends toward the coordinate origin.

The ChRM directions were also confirmed through the analysis of remagnetisation circles and show good agreement with the results obtained by principal component analysis (see Table 1 and Fig. 2, *f*, *g*). An exception is sampling site No. 4, where the anorthosite exhibits overlapping spectra of the viscous LTC and the high-temperature ChRM (see Fig. 2, *f*, *g*), complicating the identification of the latter. A similar situation is observed for specimens from Site No. 5, where the viscous component dominates, preventing the component analysis from isolating the ChRM; traces of this component are visible only through remagnetisation circle analysis (see Table 1).

Site-mean directions of the ChRM component were determined for collections from seven sites using principal component analysis (see Table 1; Fig. 2, *f*). This component exhibits bipolarity: the polarity of anorthosites from sites No. 2 and No. 4 is reversed relative to other sites. In some cases, both polarities occur within individual specimens from the same site, likely due to the prolonged cooling of large plutonic bodies, during which a geomagnetic field reversal could have occurred.

The mean ChRM directions lie in the I and III quadrants of the stereographic projection and are characterized by low inclinations (see Fig. 2, *f*). The directions show good clustering overall, except for the ChRM of anorthosites from site No. 7, which has a noticeably higher inclination of 29.8° and deviates from the general group. This deviation may result from an anomalously high degree of magnetic susceptibility anisotropy. The degree of anisotropy (P_j) for specimens from site No. 7 is 1.4 [Bakhmutov et al., 2025, Table 2, sampling site No. 16], whereas for anorthosites from other sites, P_j typically ranges from 1.05 to 1.15. Consequently, the results from site No. 7 were excluded from further palaeomagnetic pole calculations.

The mean ChRM direction for rocks from the six remaining sites (No. 1–4, 6, and 8) is: D = 214.5°, I = 4.9°, k = 200.2, α_{95} = 4.7°, N = 6. The corresponding ~1.76 Ga palaeomagnetic pole is: Φ = 29.3°, Λ = 168.2°, A_{95} = 3.3°, N = 6 (Fig. 3).

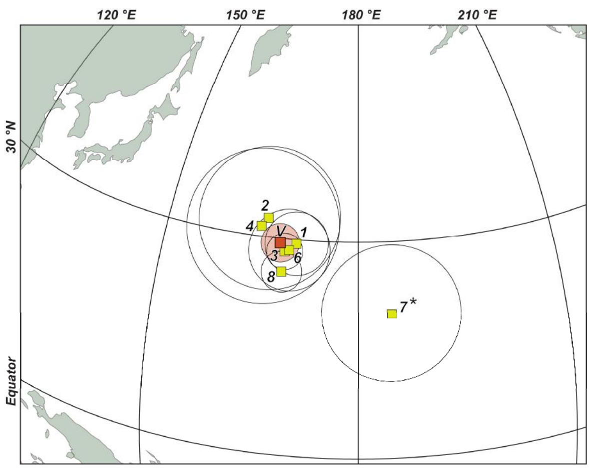

Fig. 3. New palaeomagnetic poles obtained for the basic rocks of the Volodarsk-Volynskyi massif of the Korosten pluton.

Yellow squares show the positions of the virtual geomagnetic poles with confidence intervals of A_{95}, the numbers correspond to the sampling site indexes (see Table 1 and Fig. 1, *b*); the orange square shows the palaeomagnetic pole (V). The asterisk indicates pole No. 7*, which was excluded from the calculations.

Identification of ferromagnetic minerals

Previous palaeomagnetic studies of the basic rocks from the Korosten and Korsun-Novomyrhorod plutons of the Ukrainian Shield [Mikhailova et al., 1994; Elming et al., 2001; Cherkes et al., 2023a; Bakhmutov et al., 2025] concluded that the main carrier of NRM is magnetite or titanomagnetite containing a small amount of Ti. The high-temperature ChRM component is associated with systems of oriented lamellar (needle-like) Fe–Ti oxide inclusions, which represent exsolution structures within plagioclases and pyroxenes. The presence of these structures in the respective minerals has been confirmed by optical and electron microscopy [Mikhailova et al., 1994; Cherkes et al., 2023a].

Additional rock magnetic experiments were conducted to identify the magnetic minerals. They included isothermal remanent magnetisation (IRM), thermomagnetic analysis, and the Lowrie test [Lowrie, 1990].

The results of thermal demagnetisation show that the ChRM is isolated within the T_{ub} range of 500–540–580 °C (see Table 1; Fig. 2, *a*–*c*), which is characteristic of magnetite. The IRM curves indicate that, in fields of approximately 300 mT, most specimens achieve 90–100 % saturation IRM (Fig. 4), consistent with a low-coercivity mineral such as magnetite. Additional IRM data obtained from a plagioclase monocrystal show a magnetite-like saturation curve (Fig. 4, curve with circles), suggesting that magnetite is the principal magnetic mineral among the observed systems of needle-like inclusions in plagioclases. In contrast, other specimens reach full saturation only in stronger fields (up to 0.4 T and even 1.0 T), indicating the presence of additional magnetic minerals with higher coercivity.

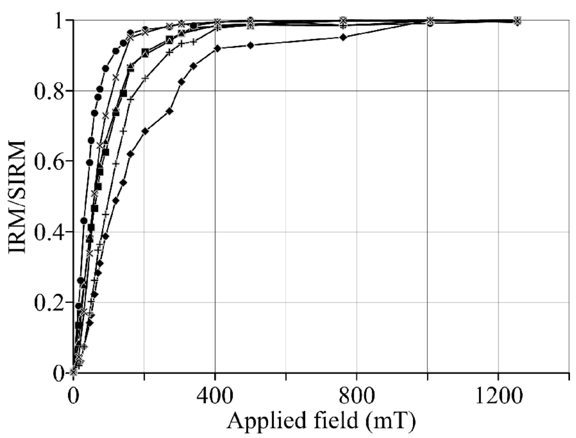

Fig. 4. Graphs of isothermal remanent magnetisation acquisition for anorthosite specimens.

IRM/SIRM is the ratio of IRM to saturation IRM. Results for a specimen of plagioclase single crystal are shown with circles.

Changes in magnetic susceptibility with temperature also indicate that the main magnetic carrier is a mineral with a Curie temperature of approximately 580 °C (Fig. 5). In most cases, the heating–cooling curves are irreversible, and new highly magnetic minerals are formed during heating. Typically, the cooling curve shows an increase in magnetic susceptibility of 10–30% (Fig. 5, *a*, *b*), while in some samples, a more pronounced increase of up to 2–5 times is observed (Fig. 5, *c*, *d*). Based on the behavior of the cooling curves, the newly formed magnetic minerals are represented by pure magnetite with a Curie temperature of about 580 °C (Fig. 5, *a*) and/or titanomagnetite containing a small amount of Ti with a Curie temperature of about 540–550 °C (Fig. 5, *b*–*d*). Titanomagnetite is occasionally detected in the heating curves (Fig. 5, *d*) and in the thermal demagnetisation data (see Fig. 2, *c*), corresponding to the T_{ub} range of the ChRM (480–550 °C).

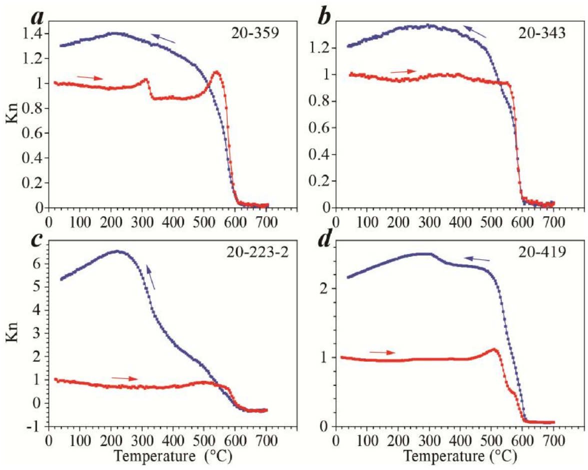

Fig. 5. Plots of normalised magnetic susceptibility (K_n) versus temperature for anorthosite (a–c) and gabbro (d) specimens.

The red and blue curves represent heating and cooling, respectively. The K_n are normalised to the initial magnetic susceptibility at 25 °C.

The results of the Lowrie test for anorthosite and gabbro show that the main portion of the IRM (approximately 80–90 % of the maximum IRM) is acquired in a 0.12 T field (Fig. 6). This soft IRM component exhibits maximum T_{ub} gradients in the range of 500–560 °C, consistent with the T_{ub} of the ChRM. The contribution of the medium and hard components generally does not exceed 10 %, and these components are also demagnetized at 550–570 °C. Considering the results from all rock magnetic analyses, it can be reasonably concluded that the main carrier of the ChRM is magnetite (or titanomagnetite with a small Ti content) with Curie temperatures of 550–580 °C.

Considering the new data together with the results of previous microscopic studies [Mikhailova et al., 1994; Cherkes et al., 2023a], it can be concluded that magnetite is the principal carrier of the ChRM. The ChRM exhibits a thermoremanent nature and is primary in both gabbros and anorthosites. Its primary origin is supported by the following evidence: 1. Bipolar, antipodal ChRM directions are observed across different sampling sites. 2. The magnetic carriers are isolated lamellar, fine-grained magnetites occurring within the exsolution structures of plagioclases and pyroxenes. 3. The newly obtained palaeomagnetic poles are in good agreement with those determined for other rocks of similar age from the Volyn and Inhul domains of the Ukrainian Shield [Mikhailova et al., 1994; Elming et al., 2001, 2010; Bakhmutov et al., 2023].

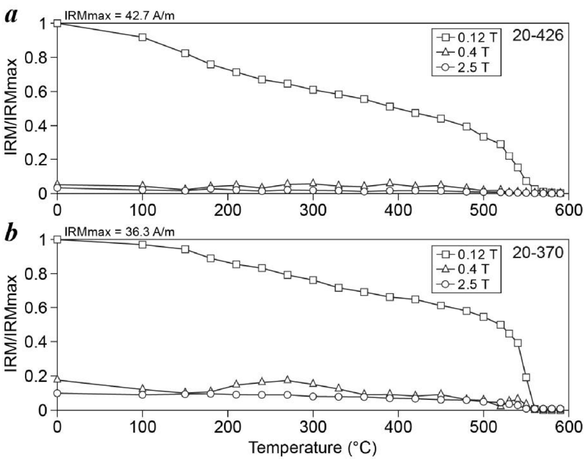

Fig. 6. Temperature demagnetisation of IRM of anorthosite (a) and gabbro (b) specimens.

Circles, triangles, and squares represent the hard, medium, and soft components of the IRM acquired in fields of 2.5 T, 0.4 T, and 0.12 T, respectively. IRM/IRM_{max} is the ratio of the IRM to the maximum value of the IRM.

Selection of palaeomagnetic poles for the Palaeoproterozoic of the EEP

The analysis of the *Global Paleomagnetic Database* [Pisarevsky, 2005], *Magnetics Information Consortium* [Jarboe et al., 2012], and *Precambrian Database PALEOMAGIA* [Veikkolainen et al., 2017], enabled to compile a selection of palaeomagnetic poles for the Palaeoproterozoic of the EEP (Baltica) and its segments. The selection includes the most reliable determinations according to the reliability criterion (*Q*) for palaeomagnetic poles [Van der Voo, 1990].

For Sarmatia, the selection comprises 11 poles spanning an age range of 2078–1720 Ma (Fig. 7, red). The apparent polar wander path (APWP) begins with poles No. 1 and 2, dated to about 2.07 Ga, which gradually shift toward poles NM (2035 Ma, Novoukrainka Massif of the Inhul domain of the Ukrainian Shield) and BM (1987 Ma, Buky Massif of the Volyn domain of the Ukrainian Shield), as well as pole No. 3, derived from dykes in the north-western part of the Volyn megablock of the Ukrainian Shield. The consistency among these poles – determined from rocks of the Volyn and Inhul domains – suggests that these blocks have remained stationary relative to each other since ~2.0 Ga. After 2 Ga, palaeomagnetic data for the Sarmatian segment of the APWP are absent for roughly 250 Myr (Fig. 7, red dotted APWP line). According to geological evidence, the assembly of Volgo-Sarmatia, resulting from the collision between Sarmatia and Volgo-Uralia, occurred between 2.1–2.0 Ga [Bogdanova et al., 2005]. Consequently, Sarmatia is further considered part of Volgo-Sarmatia.

The APWP of Sarmatia continues with a well-clustered group of poles–KP, KNP, and No. 4–6-dated to 1.76–1.74 Ga. Except for the KNP pole, these were obtained from rocks of the Volyn domain of the Ukrainian Shield. Similar to the ~2.0 Ga BM and NM poles, the KP (1760 Ma, Korosten pluton of the Volyn domain) and KNP (1750 Ma, Korsun-Novomyrhorod pluton of the Inhul domain) poles are closely positioned, indicating that these domains have maintained a fixed relative position since at least 1.76–1.75 Ga.

Considering the agreement among poles KP, KNP, and No. 4–6, as well as the presence of a positive baked contact test for pole No. 4 [Elming et al., 2010], this group of poles can be regarded as the key and most reliable dataset for the Palaeoproterozoic of Sarmatia. This section of the APWP terminates with pole No. 7 (1720 Ma), which is slightly displaced toward the equator. No younger determinations are available for the Sarmatian segment of the APWP.

According to geological and tectonic data, the formation of Baltica, resulting from the amalgamation of Fennoscandia and Volgo-Sarmatia, occurred around 1.7 Ga [Bogdanova et al., 2005]. Therefore, the APWPs of Sarmatia and Fennoscandia are subsequently continued by the APWP of Baltica (Fig. 7, green).

The selection for Fennoscandia includes 26 determinations within the age range of 2449–1700 Ma (Fig. 7, blue), most of which fall between 1800 and 1750 Ma. In the interval 2.45–1.97 Ga, the APWP contains significant gaps and is represented by only five individual determinations – two ~2450 Ma poles (No. 8 and 9), a 2295 Ma pole (No. 10), and poles No. 11 and 12 dated to 2058 Ma and 1970 Ma, respectively. Because of the absence of palaeomagnetic data for the ~150 Myr interval between poles No. 8–9 and No. 10, as well as the ~240 Ma and ~90 Ma gaps between poles No. 10 and 11, and No. 11 and 12, respectively, the Fennoscandian APWP segment for 2.49–1.97 Ga cannot be regarded as reliable.

Table 2

Selected palaeomagnetic poles for the Palaeoproterozoic of the EEP (Baltica) and its segments

No.	Age (Ma)	Φ (°)	Λ (°)	A_{95} (°)	*Q*	Reference
Sarmatia						
1	2078	12.0	172.0	5.0	4	Iosifidi et al., 1999
2	2067	15.7	182.9	12.4	4	Elming et al., 2010
NM	2035	43.4	141.9	6.2	4	Cherkes et al., 2023b
3	2000	64.4	140.4	12.7	4	Elming et al., 2010
BM	1987	47.5	144.9	5.2	4	Cherkes et al., 2023a
4	1765	28.8	169.8	4.4	7	Elming et al., 2010
5	1760	30.2	177.6	2.8	6	Kravchenko, 2005
KP	1760	26.7	169.6	4.2	6	this paper; Bakhmutov et al., 2023
KNP	1750	22.7	167.4	3.3	6	Bakhmutov et al., 2023
6	1740	20.5	167.4	5.6	6	Elming et al., 2001
7	1720	10.7	163.2	10.2	5	Elming et al., 2010
Fennoscandia						
8	2449	-12.7	247.5	9.6	5	Shcherbakova et al., 2017
9	2446	-19.9	278.7	6.1	5	Mertanen et al., 1999
10	2295	-17.4	262.3	9.8	6	Mertanen et al., 2006b
11	2058	24.7	300.8	16.4	6	Torsvik and Meert, 1995
12	1970	44.4	101.5	6.3	5	Lubnina et al., 2017
13	1931	40.2	247.3	6.0	4	Mertanen and Pesonen, 1994
14	1890	42.6	227.9	4.9	3	Elming, 1985
15	1885	46.9	237.5	3.5	5	Luoto et al., 2023
16	1870	45.7	230.9	5.5	7	Klein et al., 2016
17	1860	54.7	234.7	5.2	5	Veselovskiy et al., 2019
18	1806	43.0	220.0	2.8	5	Elming, 1985
19	1800	49.0	209.0	3.9	5	Elming, 1994
20	1800	50.9	229.1	7.2	4	Mertanen et al., 2006a
21	1786	43.0	233.3	10.9	6	Elming et al., 2009
22	1777	45.7	182.7	8.0	7	Pisarevsky and Bylund, 2010
23	1775	39.7	221.1	4.0	6	Pisarevsky and Sokolov, 2001
24	1775	45.8	218.0	4.9	4	Damm et al., 1997
25	1770	39.7	221.1	4.0	7	Pisarevsky and Sokolov, 2001
26	1767	50.4	222.2	10.2	4	Veselovskiy et al., 2013
27	1751	39.1	216.6	6.7	5	Fedotova et al., 1999
28	1751	40.5	229.8	8.1	4	Fedotova et al., 1999
29	1751	36.2	208.6	5.8	4	Fedotova et al., 1999
30	1751	40.5	227.3	7.5	4	Khramov et al., 1997
31	1751	33.9	214.3	7.3	4	Khramov et al., 1997
32	1751	37.8	210.6	5.5	4	Damm et al., 1997
33	1700	51.6	220.2	4.8	5	Elming et al., 2019
Baltica						
34	1642	26.0	209.0	11.0	6	Salminen et al., 2021
35	1639	28.0	172.0	8.0	3	Salminen et al., 2019
36	1633	26.4	180.0	9.4	4	Mertanen and Pesonen, 1995
37	1630	30.2	175.4	9.4	3	Neuvonen, 1986
38	1614	22.0	147.0	14.0	4	Elming et al., 2009

Note: No. is the index of the palaeomagnetic pole according to Fig. 7; Φ and Λ are latitude and longitude of the palaeomagnetic pole, respectively; A_{95} is the radius of the confidence circle of the palaeomagnetic pole at 95% probability level; *Q* is the reliability criterion for palaeomagnetic determinations [Van der Voo, 1990].

From pole No. 12, the APWP shifts ~90° westward along a great circle to pole No. 13 (1931 Ma), near which there is a relatively dense cluster of poles (No. 14–32) covering the 1890–1751 Ma range. It can be inferred that during the period between 1.9 Ga and 1.75 Ga, Fennoscandia did not undergo significant latitudinal drift or rotation. The group of poles No. 22–32, dated to 1777–1751 Ma, may therefore represent the key interval for Fennoscandia around ~1.76 Ga. These poles show good mutual consistency, and poles No. 22 and 25 are further supported by positive field test results [Pisarevsky and Bylund, 2010; Pisarevsky and Sokolov, 2001]. The Fennoscandian APWP terminates with the youngest pole, No. 33 (1700 Ma), which also lies within the aforementioned cluster.

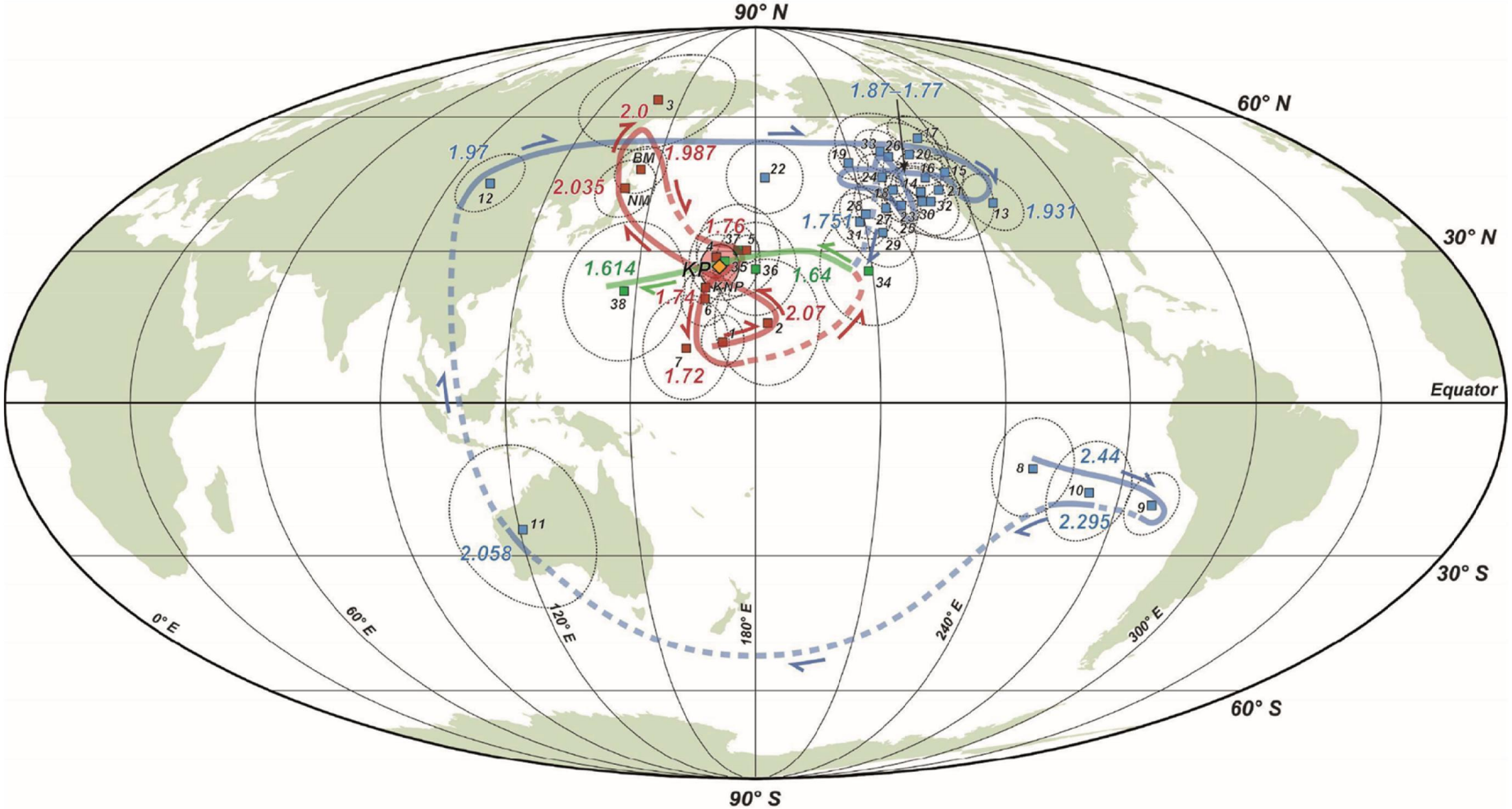

Fig. 7. Selected palaeomagnetic determinations and a model of the apparent polar wander path for the Palaeoproterozoic of Baltica.

Red, blue, and green squares show the positions of the palaeomagnetic poles for Sarmatia, Fennoscandia, and Baltica, respectively. Orange rhombus is the new determination (KP) for the Korosten pluton of the Ukrainian Shield. The corresponding A_{95} confidence circles are shown around the poles with a dashed line (for the new pole, the A_{95} interval is filled in red). The black indexes near the poles correspond to the indexes in Table 2. The red, blue, and green thick lines show the APWP for Sarmatia, Fennoscandia, and Baltica, respectively; the dashed thick line indicates interpolated/unreliable APWP sections. Large numbers of the corresponding colour near the APWP indicate the age of the APWP in Ga.

There is a gap of approximately 60 Myr between the youngest poles of Sarmatia (pole No. 7, 1720 Ma) and Fennoscandia (pole No. 33, 1700 Ma) and the chronologically subsequent pole No. 34 of Baltica (1645 Ma). The younger Palaeoproterozoic poles of Baltica (No. 34–38, dated 1645–1614 Ma) were obtained exclusively from rocks of the Fennoscandian segment of the EEP. The youngest comparable poles of Fennoscandia (No. 22–32) and Sarmatia (No. 4–6, KP, KNP), dated to about 1.75–1.77 Ga, form distinct and separate groups (Table 2; Fig. 7). Thus, according to palaeomagnetic data, the amalgamation of the Baltica palaeocontinent occurred no earlier than 1.75–1.76 Ga (based on the most reliable section of the APWP) and possibly not earlier than 1.72–1.70 Ga if individual determinations No. 7 and No. 33 are taken into account.

Note: No. is the index of the palaeomagnetic pole according to Fig. 7; Φ and Λ are latitude and longitude of the palaeomagnetic pole, respectively; A_{95} is the radius of the confidence circle of the palaeomagnetic pole at 95% probability level; *Q* is the reliability criterion for palaeomagnetic determinations [Van der Voo, 1990].

The lower time limit for the assembly of Baltica is constrained solely by geological data and is estimated at approximately 1.7 Ga [Bogdanova et al., 2005]. Poles younger than this age are attributed to the Baltica palaeocontinent. The Palaeoproterozoic section of the Baltica APWP (see Fig. 7, green) is represented by poles No. 34–38, corresponding to ages between 1642–1614 Ma. Among these, pole No. 34 is the most reliable, as it is supported by a positive field test result [Salminen et al., 2021].

Palaeogeographic reconstruction of the EEP in the Palaeoproterozoic

Palaeogeographic reconstructions of the Ukrainian Shield (as part of Sarmatia) and Fennoscandia were performed based on a selection of palaeomagnetic poles and the APWP for the Palaeoproterozoic of the EEP, covering the age range 2.78–1.614 Ga (see Table 2 and Fig. 7). Calculations of palaeolatitudes and latitudinal drift rates for the Baltica palaeocontinent and its segments (Sarmatia and Fennoscandia) are presented in Fig. 8, while reconstructions for specific time intervals are shown in Fig. 9. Because the proposed APWP for the Palaeoproterozoic of Baltica has no clear connection with the APWP for later epochs, it is impossible to establish the polarity of the palaeomagnetic poles clearly. In our case, the APWP was calculated based on the principle of the minimum distance between chronologically closest poles corresponding to reasonable rates of latitudinal drift and angular rotation. The palaeomagnetic poles from Table 2 were accepted as northern poles. For the interval 2.44–1.97 Ga (poles No. 8–12), there is insufficient data to calculate the APWP for Fennoscandia, so it is impossible to establish the polarity of these poles relative to the younger section.

According to the selection (see Table 2) and calculations of the kinematic parameters of the EEP (Fig. 8), the general features of the palaeotectonic evolution of the EEP and its segments during the Palaeoproterozoic can be summarized as follows.

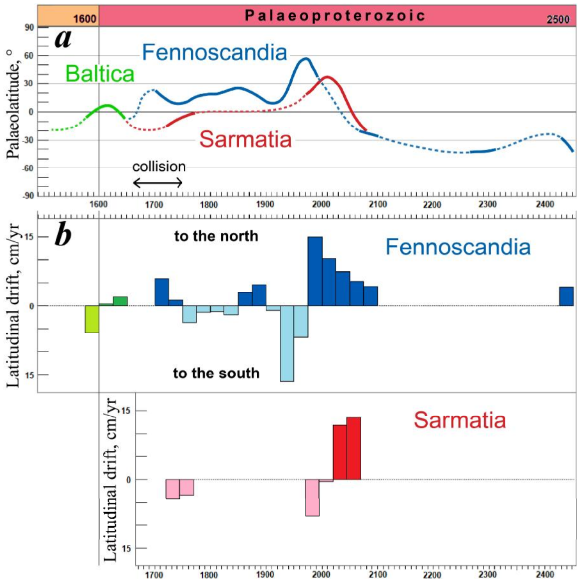

Fig. 8. Palaeolatitudinal position (a) and latitudinal drift rates (b) of Sarmatia (red), Fennoscandia (blue), and Baltica (green).

The palaeolatitude (a) of Sarmatia, Fennoscandia, and the Baltica is shown by solid lines in red, blue, and green, respectively; dashed sections indicate the absence of data. The darker and lighter colours show the direction of drift (b) of the tectonic blocks to the north or to the south, respectively.

According to individual palaeomagnetic determinations, around 2.45 Ga (poles No. 8, 9), 2.295 Ga (pole No. 10), and 2.058 Ga (pole No. 11), Fennoscandia was located at middle to subequatorial latitudes in the southern hemisphere (Figs. 8–9). Subsequently, Fennoscandia drifted northward at an average latitudinal drift rate of about 8 cm/yr, reaching polar latitudes in the northern hemisphere by approximately 1.97 Ga (pole No. 12; Fig. 9). Afterward, it migrated toward the equator at an average drift rate of ~10 cm/yr and an angular clockwise rotation rate of ~2.8 °/Myr. Between 1.93 Ga and 1.75 Ga (poles No. 13–32), Fennoscandia stabilized in subequatorial latitudes of the northern hemisphere (Fig. 8) and did not undergo significant latitudinal shifts or rotations.

Between 2.078 Ga and 1.987 Ga, Sarmatia shifted from subequatorial latitudes of the southern hemisphere (poles No. 1, 2) to middle latitudes of the northern hemisphere (poles No. 3, NM, BM) at a latitudinal drift rate of ~10 cm/year (Figs. 8–9), with an average angular rotation rate not exceeding 0.5 °/Ma. Around the same time (2.1–2.0 Ga), Sarmatia and Volgo-Uralia collided, forming a larger continental block known as Volgo-Sarmatia [Bogdanova et al., 2005].

No palaeomagnetic data are available for Sarmatia between 2.0 and 1.76 Ga (poles KP, KNP, and poles No. 4, 5). At approximately 1.76 Ga, Sarmatia and Fennoscandia occupied equatorial latitudes, with Sarmatia rotated ~40° counterclockwise relative to Fennoscandia (Fig. 9). Insufficient data exist to determine the relative positions of Fennoscandia and Sarmatia (Volgo-Sarmatia) during the 1.75–1.64 Ga interval. From around 1.7 Ga onward, Sarmatia and Fennoscandia evolved within the unified structure of the Baltica palaeocontinent [Bogdanova et al., 2005]. By approximately 1.63 Ga (poles No. 34–38), Baltica occupied equatorial latitudes (Fig. 9).

The new determination (KP) refines and extends the results of previous studies on the rocks of the Korosten pluton [Elming et al., 2001; Kravchenko, 2005], providing greater detail for the Palaeoproterozoic section of the Sarmatia APWP (see Fig. 7; Table 2). The new data align well with findings from palaeomagnetic studies on dyke rocks of similar age located in northwestern part of the Volyn domain of the Ukrainian Shield [Elming et al., 2010] and on rocks from the Korsun-Novomyrhorod massif of the Inhul domain of the Ukrainian Shield [Bakhmutov et al., 2023]. Palaeogeographic reconstructions for the 1.76–1.75 Ga interval (Fig. 9), for which representative palaeomagnetic data are available for both Fennoscandia and Sarmatia, generally support earlier estimates [Elming et al., 2010; Lahtinen et al., 2023]. Thus, according to palaeomagnetic evidence, the amalgamation of Fennoscandia and Volgo-Sarmatia–and the subsequent formation of the Baltica palaeocontinent–occurred no earlier than 1.75–1.76 Ga.

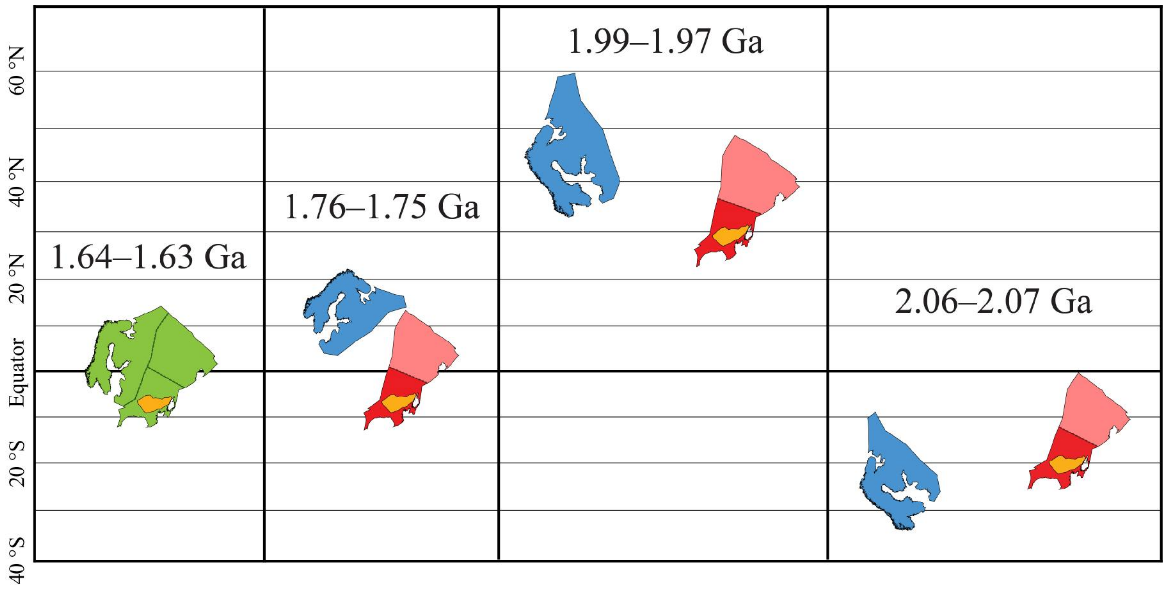

Fig. 9. Palaeogeographic models of the Baltica and its segments in the Palaeoproterozoic based on palaeomagnetic data.

Fennoscandia is shown in blue, Sarmatia in red, Volgo-Uralia in pink, and the Baltica in green. Location of the Ukrainian Shield within Sarmatia/Baltica is shown in orange.

Scientific novelty

New palaeomagnetic determinations for Palaeoproterozoic rocks of the Ukrainian Shield, along with additional data on the magnetic mineral properties of the basic rocks of the Korosten pluton, have been obtained. A selection of the most reliable palaeomagnetic determinations for the EEP during the Palaeoproterozoic was compiled, and a model of the APWP was constructed. Based on this APWP, the corresponding kinematic parameters were calculated, and palaeogeographic reconstructions were developed.

Practical significance

The results provide detailed insights into the geodynamic evolution of the EEP during the Palaeoproterozoic and can be applied in palaeogeographic reconstructions.

Conclusions

The basic rocks of the VVM (anorthosites and gabbros) of the Korosten plutonic complex are informative for palaeogeographic reconstructions based on palaeomagnetic data. According to rock magnetic and microscopic analyses, the carriers of the ChRM are isolated lamellar and needle-like, oriented exsolution systems of magnetite and titanomagnetite within plagioclases and pyroxenes. The bipolar ChRM of the studied anorthosite and gabbro specimens is isolated within the T_{ub} range of approximately 470–580 °C. The viscous LTC, demagnetized up to 350–450 °C, aligns closely with the direction of the PEMF at the sampling site.

The new results are consistent with those obtained by other authors for rocks of similar age from the Ukrainian Shield. The new palaeomagnetic pole for the VVM rocks, calculated using the ChRM of anorthosite and gabbro specimens from six sampling sites, has the following parameters: Φ = 29.3°, Λ = 168.2°, A_{95} = 3.3°, N = 6.

The new palaeomagnetic determination for the Volyn domain of the Ukrainian Shield is consistent with palaeomagnetic data from rocks of the same age in the Inhul domain, indicating that these domains developed as a single tectonic unit within the Ukrainian Shield since at least 1.76 Ga.

According to the selected palaeomagnetic determinations for the Palaeoproterozoic of the EEP, the final amalgamation of Fennoscandia and Sarmatia occurred no earlier than 1.76 Ga. At that time, both Fennoscandia and Sarmatia were situated near the equatorial region, with Sarmatia rotating ~40° counterclockwise relative to Fennoscandia compared with their present-day positions within the EEP.

Acknowledgments

The author expresses sincere gratitude to V. G. Bakhmutov for managing the research and fieldwork, as well as for his valuable advice and comments on this paper; to O. V. Mitrokhin for professional support during fieldwork and geological consultations; and to I. B. Poliachenko for significant assistance in the field. The author is also grateful to T. V. Skarboviichuk and L. M. Diachuk for their help with laboratory measurements, and to V. V. Shpyra for assistance with specimen preparation. This research was carried out as part of the state-funded project *"Geodynamics of the south-western part of the East European Platform based on palaeomagnetic data"* (state registration number 0119U000079) at the Institute of Geophysics of the National Academy of Sciences of Ukraine.

References

Bakhmutov, V. G., Poliachenko, I. B., & Cherkes, S. I. (2018). Problems of palaeomagnetism of the Precambrian of the territory of Ukraine. *Geophysical Journal, 40*(5), 245–268. https://doi.org/10.24028/gzh.0203-3100.v40i5.2018.147491 (in Russian).

Bakhmutov, V., Mytrokhyn, O., Poliachenko, I., & Cherkes, S. (2023). New palaeomagnetic data for Palaeoproterozoic AMCG complexes of the Ukrainian Shield. *Geofizicheskiy Zhurnal, 45*(4), 3–19. https://doi.org/10.24028/gj.v45i4.286283

Bakhmutov, V., Mytrokhyn, O., Cherkes, S., & Poliachenko, I. (2025). Magnetism and anisotropy of magnetic susceptibility of gabbroids of the Volodarsk-Volynskyi massif of the Korosten pluton of the Ukrainian Shield. *Geofizicheskiy Zhurnal, 47*(4). https://doi.org/10.24028/gj.v47i4.335689

Bogdanova, S. V., Pashkevich, I. K., Buryanov, V. B., Makarenko, I. A., Orlyuk, M. I., Skobelev, V. M., Starostenko, V. I., & Legostaeva, O. V. (2004). The 1.80–1.74 Ga gabbro-anorthosite-rapakivi Korosten Pluton in the NW Ukrainian Shield: a 3-D geophysical reconstruction of deep structure. *Tectonophysics, 381*(1–4), 5–27. https://doi.org/10.1016/j.tecto.2003.10.023.

Bogdanova, S. V., Gorbatschev, R. G., & Garetsky, R. G. (2005). The East European Craton. In: R. C. Selley, L. R. Cocks, I. R. Plimer (Eds.), *Encyclopedia of Geology* (Vol. 2, pp. 34–49). Elsevier. https://doi.org/10.1016/B0-12-369396-9/00426-3

Buchan, K. L. (2013). Key paleomagnetic poles and their use in Proterozoic continent and supercontinent reconstructions: A review. *Precambrian Research, 238*, 93–110. https://doi.org/10.1016/j.precamres.2013.09.018

Chadima, M., & Hrouda, F. (2006). Remasoft 3.0 a user-friendly paleomagnetic data browser and analyzer. *Travaux Géophysiques, 27*, 20–21.

Cherkes, S., Bakhmutov, V., Mytrokhyn, O., Poliachenko, I., & Skarboviychuk, T. (2023). Palaeomagnetism of the Palaeoproterozoic basic rocks of the Volodarsk-Volynskyi massif, Korosten plutonic complex. In *International Conference of Young Professionals "GeoTerrace-2023"* (Vol. 2023, GeoTerrace-2023-008). European Association of Geoscientists & Engineers. https://doi.org/10.3997/2214-4609.2023510008.

Cherkes, S., Bakhmutov, V., Poliachenko, I., Mytrokhyn, O., Shpyra, V., & Yakukhno, V. (2023). Palaeomagnetism of the Palaeoproterozoic Rocks of the ~2 Ga Novoukrainka and Buky Massifs of the Ukrainian Shield. In *17th International Conference Monitoring of Geological Processes and Ecological Condition of the Environment* (Vol. 2023, Mon23-199). European Association of Geoscientists & Engineers. https://doi.org/10.3997/2214-4609.2023520199

Damm, V., Gendler, T. S., Gooskova, E. G., Khramov, A. N., Lewandowski, M., Nozharov, P., Pavlov, V. I., Petrova, G. N., Pisarevsky, S. A., & Sokolov, S. J. (1997). Palaeomagnetic studies of Proterozoic rocks from the Lake Onega region, southeast Fennoscandian Shield. *Geophysical Journal International*, *129*(3), 518–530. https://doi.org/10.1111/j.1365-246X.1997.tb04491.x

Elming, S.-Å. (1985). A palaeomagnetic study of Svecokarelian basic rocks from northern Sweden. *Geologiska Föreningen i Stockholm Förhandlingar*, *107*(1), 17–35. https://doi.org/10.1080/11035898509452608

Elming, S.-Å. (1994). Palaeomagnetism of Precambrian rocks in northern Sweden and its correlation to radiometric data. *Precambrian Research*, *69*(1–4), 61–79. https://doi.org/10.1016/0301-9268(94)90079-5

Elming, S.-Å., & Mattsson, H. (2001). Post Jotnian basic Intrusions in the Fennoscandian Shield, and the break up of Baltica from Laurentia: a palaeomagnetic and AMS study. *Precambrian Research*, *108*(3–4), 215–236. https://doi.org/10.1016/S0301-9268(01)00131-0

Elming, S.-Å., Moakhar, M.O., Layer, P., & Donadini, F. (2009). Uplift deduced from remanent magnetization of a proterozoic basic dyke and the baked country rock in the Hoting area, Central Sweden: a palaeomagnetic and ^{40}Ar/^{39}Ar study. *Geophysical Journal International*, *179*(1), 59–78. https://doi.org/10.1111/j.1365-246X.2009.04265.x

Elming, S.-Å., Shumlyanskyy, L., Kravchenko, S., Layer, P., & Söderlund, U. (2010). Proterozoic Basic dykes in the Ukrainian Shield: A palaeomagnetic, geochronologic and geochemical study – The accretion of the Ukrainian Shield to Fennoscandia. *Precambrian Research, 178*(1-4), 119–135. https://doi.org/10.1016/j.precamres.2010.02.001

Elming, S.-Å., Layer, P., & Söderlund, U. (2019). Cooling history and age of magnetization of a deep intrusion: A new 1.7 Ga key pole and Svecofennian-post Svecofennian APWP for Baltica. *Precambrian Research*, *329*, 182–194. https://doi.org/10.1016/j.precamres.2018.05.022

Fedotova, M. A., Khramov, A. N., Pisakin, B. N., & Priyatkin, A. A. (1999). Early Proterozoic palaeomagnetism: new results from the intrusives and related rocks of the Karelian, Belomorian and Kola provinces, eastern Fennoscandian Shield. *Geophysical Journal International, 137*(3), 691–712. https://doi.org/10.1046/j.1365-246x.1999.00817.x

Halls, H. C. (1976). A Least-Squares Method to find a Remanence Direction from Converging Remagnetization Circles. *Geophysical Journal International*, *45*(2), 297–304. https://doi.org/10.1111/j.1365-246X.1976.tb00327.x

Iosifidi, A. G., Bogdanova, S., Khramov, A. N., & Bylund, G. (1999). Palaeomagnetic study of Palaeoproterozoic granitoids from the Voronezh Massif, Russia. *Geophysical Journal International*, *137*(3), 723–731. https://doi.org/10.1046/j.1365-246x.1999.00818.x

Jarboe, N. A., Koppers, A. A., Tauxe, L., Minnett, R., & Constable, C. (2012). The Online MagIC Database: Data Archiving, Compilation, and Visualization for the Geomagnetic, Paleomagnetic and Rock Magnetic Communities. In *American Geophysical Union Fall Meeting 2012* (GP31A-1063). American Geophysical Union.

Khramov, A. N., Fedotova, M. A., Pisakin, B. N., & Priyatkin, A. A. (1997). Paleomagnetism of Early Proterozoic intrusions and associated rocks of Karelia and the Kola Peninsula: Contribution to the development of a model for the Precambrian evolution of the Russian-Baltic craton. *Fizika Zemli*, *(6)*, 24–41. (in Russian)

Kirschvink, J. L. (1980). The least-squares line and plane and the analysis of palaeomagnetic data. *Geophysical Journal International*, *62*(3), 699–718. https://doi.org/10.1111/j.1365-246X.1980.tb02601.x

Klein, R., Pesonen, L. J., Mänttäri, I., & Heinonen, J. S. (2016). A late Paleoproterozoic key pole for the Fennoscandian Shield: A paleomagnetic study of the Keuruu diabase dykes, Central Finland. *Precambrian Research*, *286*, 379-397. https://doi.org/10.1016/j.precamres.2016.10.013

Kravchenko, S. N. (2005). First estimate for the age of a mesoproterozoic palaeomagnetic pole from the Volodarsk-Volynsky Massif, The Ukrainian Shield. *Studia Geophysica et Geodaetica*, *49*, 177–190. https://doi.org/10.1007/s11200-005-0004-6

Lahtinen, R., Köykkä, J., Salminen, J., Sayab, M., & Johnston, S.T. (2023). Paleoproterozoic tectonics of Fennoscandia and the birth of Baltica. *Earth-Science Reviews*, *246*, 104586. https://doi.org/10.1016/j.earscrev.2023.104586

Lowrie, W. (1990). Identification of ferromagnetic minerals in a rock by coercivity and unblocking temperature properties. *Geophysical Research Letters*, *17*(2), 159–162. https://doi.org/10.1029/GL017I002p00159

Lubnina, N. V., Pisarevsky, S. A., Stepanova, A. V., Bogdanova, S. V., & Sokolov, S. J. (2017). Fennoscandia before Nuna/Columbia: Paleomagnetism of 1.98–1.96 Ga mafic rocks of the Karelian craton and paleogeographic implications. *Precambrian Research*, *292*, 1–12. https://doi.org/10.1016/j.precamres.2017.01.011

Luoto, T., Salminen, J., Mertanen, S., Elming, S. Å., & Pesonen, L. J. (2023). New palaeoproterozoic palaeomagnetic data from Central and Northern Finland indicate a long-lived stable position for Fennoscandia. *Geophysical Journal International*, *235*(2), 1810–1831. https://doi.org/10.1093/gji/ggad247

Mertanen, S., & Pesonen, L. J. (1994). Preliminary results of a palaeomagnetic and rock magnetic study of the Proterozoic Tsuomasvarri intrusions, northern

Fennoscandia. *Precambrian Research*, *69*(1–4), 25–50. https://doi.org/10.1016/0301-9268(94)90077-9

Mertanen, S., & Pesonen, L. J. (1995). Palaeomagnetic and rock magnetic investigations of the Sipoo Subjotnian quartz porphyry and diabase dykes, southern Fennoscandia. *Physics of the Earth and Planetary Interiors*, *88*(3–4), 145–175. https://doi.org/10.1016/0031-9201(94)02992-K

Mertanen, S., Halls, H. C., Vuollo, J. I., Pesonen, L. J., & Stepanov, V. S. (1999). Paleomagnetism of 2.44 Ga mafic dykes in Russian Karelia, eastern Fenno-scandian Shield – implications for continental recon-structions. *Precambrian Research*, *98*(3–4), 197–221. https://doi.org/10.1016/S0301-9268(99)00050-9

Mertanen, S., Eklund, O., Shebanov, A., Frank-Kamenetsky, D., & Vasilieva, T. (2006a). Paleo- and mesoproterozoic dyke swarms in the Lake Ladoga area, NW Russia – palaeomagnetic studies. In E. Hanski, S. Mertanen, O.T. Ramo, & J. Vuollo (Eds.), *Dyke Swarms – Time Markers of Crustal Evolution* (pp. 63–74). Taylor & Francis.

Mertanen, S., Holtta, P., Pesonen, L. J., & Paavola, J. (2006b). Palaeomagnetism of palaeoproterozoic dolerite dykes in central Finland. In E. Hanski, S. Mertanen, O.T. Ramo, & J. Vuollo (Eds.), *Dyke Swarms – Time Markers of Crustal Evolution* (pp. 243–256). Taylor & Francis.

Mikhailova, N. P., Kravchenko, S. N., & Glevasskaia, A. M. (1994). *Paleomagnetism of anorthosites*. Kyiv: Naukova Dumka. (in Russian).

Müller, R. D., Cannon, J., Qin, X., Watson, R. J., Gurnis, M., Williams, S., Pfaffelmoser, T., Seton, M., Russell, S. H. J., & Zahirovic S. (2018). GPlates: Building a virtual Earth through deep time. *Geochemistry, Geophysics, Geosystems, 19*(7), 2243–2261. https://doi.org/10.1029/2018GC007584

Mytrokhyn, O. V. (2011). *Anothosite-rapakivi-granite association of Ukrainian Shield (geology, composition and origin)* (Doctoral dissertation). Available from National Repository of Academic Texts (RN 0511U000260). (in Ukrainian)

Mytrokhyn, O., Bilan, O., & Hrushchynska, O. (2011). Manifestations of contact metamorphism in the rocks of the ancient "frame" of the Korosten pluton. *Visnyk of Taras Shevchenko National University of Kyiv. Geology*, *54*, 19–23. http://www.library.univ.kiev.ua/ukr/host/10.23.10.100/db/ftp/visnyk/geolog_54_2011.pdf (in Ukrainian)

Neuvonen, K. J. (1986). On the direction of remanent magnetization of the quartz porphyry dikes in SE Finland. *Bulletin of Geological Survey of Finland*, *58*(1–2), 195–201. https://doi.org/10.17741/bgsf/58.1.013

Pisarevsky, S. A., & Sokolov, S. J. (2001). The magnetostratigraphy and a 1780 Ma palaeomagnetic pole from the red sandstones of the Vazhinka River section, Karelia, Russia. *Geophysical Journal International, 146*(2), 531–538. https://doi.org/10.1046/j.0956-540x.2001.01479.x

Pisarevsky, S. (2005). New edition of the Global Paleomagnetic Database. *Eos, Transactions AGU*, *86*(17), 170. https://doi.org/10.1029/2005EO170004

Pisarevsky, S. A., & Bylund, G. (2010). Paleomagnetism of 1780–1770 Ma Mafic and Composite Intrusions of Småland (Sweden): Implications for the Mesoproterozoic Supercontinent. *American Journal of Science*, *310*(9), 1168–1186. https://doi.org/10.2475/09.2010.15

Salminen, J., Klein, R., & Mertanen, S. (2019). New rock magnetic and paleomagnetic results for the 1.64 Ga Suomenniemi dyke swarm. SE Finland. *Precambrian Research*, *329*, 195–210. https://doi.org/10.1016/j.precamres.2018.01.001

Salminen, J., Elming, S. Å., Mertanen, S., Wang, C., Almqvist, B., & Moakhar, M. O. (2021). Paleomagnetic studies of rapakivi complexes in the Fennoscandian shield – Implications to the origin of Proterozoic massif-type anorthosite magmatism. *Precambrian Research*, *365*, 106406. https://doi.org/10.1016/j.precamres.2021.106406

Shcherbakova, V. V., Lubnina, N. V., Shcherbakov, V. P., Zhidkov, G. V., & Tsel'movich, V. A. (2017). Paleointensity determination on Neoarchaean dikes within the Vodlozerskii terrane of the Karelian craton. *Izvestiya, Physics of the Solid Earth*, *53*, 714–732. https://doi.org/10.1134/S1069351317050111

Shumlyanskyy, L. V. (2012). *Petrology and geo-chronology of rock complexes of the north-west region of the Ukrainian shield and its western slope* (Doctoral dissertation). Available from National Repository of Academic Texts (RN 0512U000865). (in Ukrainian)

Shumlyanskyy, L., Hawkesworth, C., Billström, K., Bogdanova, S., Mytrokhyn, O., Romer, R., Dhuime, B., Claesson, S., Ernst, R., Whitehouse, M., & Bilan, O. (2017). The origin of the Palaeoproterozoic AMCG complexes in the Ukrainian shield: New U-Pb ages and Hf isotopes in zircon. *Precambrian Research*, *292*, 216–239. https://doi.org/10.1016/j.precamres.2017.02.009

Torsvik, T. H., & Meert, J. G. (1995). Early Proterozoic palaeomagnetic data from the Pechenga Zone (north-west Russia) and their bearing on Early Proterozoic palaeogeography. *Geophysical Journal International*, *122*(2), 520–536. https://doi.org/10.1111/j.1365-246X.1995.tb07011.x

Torsvik, T. H., & Smethurst, M. A. (1999). Plate tectonic modelling: virtual reality with GMAP. *Computers and Geosciences, 25*(4), 395–402. https://doi.org/10.1016/s0098-3004(98)00143-5

Van der Voo, R. (1990). The reliability of paleomagnetic data. *Tectonophysics, 184*(1), 1–9. https://doi.org/10.1016/0040-1951(90)90116-P

Veikkolainen, T. H., Biggin, A. J., Pesonen, L. J., Evans, D. A., & Jarboe, N. A. (2017). Advancing Precambrian palaeomagnetism with the PALEOMAGIA and PINT (QPI) databases. *Scientific Data*, *4*, 170068. https://doi.org/10.1038/sdata.2017.68

Veselovskiy, R. V., Arzamastsev, A. A., Demina, L. I., Travin, A. V., & Botsyun, S. B. (2013). Paleomagnetism, geochronology, and magnetic mineralogy of Devonian dikes from the Kola alkaline province (NE Fennoscandian Shield). *Izvestiya, Physics of the Solid Earth*, *49*, 526–547. https://doi.org/10.1134/S106935131303018X

Veselovskiy, R. V., Samsonov, A. V., Stepanova, A. V., Salnikova, E. B., Larionova, Y. O., Travin, A. V., Arzamastsev, A. A., Egorova, S. V., Erofeeva, K. G., Stifeeva, M. V., Shcherbakova, V. V., Shcherbakov, V. P., Zhidkov, G. V., & Zakharov, V. S. (2019). 1.86 Ga key paleomagnetic pole from the Murmansk craton intrusions – Eastern Murman Sill Province, NE Fennoscandia: Multidisciplinary approach and paleotectonic applications. *Precambrian Research, 324*, 126–145. https://doi.org/10.1016/j.precamres.2019.01.017

Семен ЧЕРКЕС[1]

[1]Інститут геофізики ім. С. І. Субботіна Національної академії наук України, просп. Академіка Палладіна, 32, Київ, 03142, Україна, тел. +38(050)1565912, ел. пошта SemyonCherkes@gmail.com

НОВІ РЕЗУЛЬТАТИ ПАЛЕОМАГНІТНИХ ТА ПЕТРОМАГНІТНИХ ДОСЛІДЖЕНЬ ГАБРОЇДІВ КОРОСТЕНСЬКОГО ПЛУТОНУ УКРАЇНСЬКОГО ЩИТА

Виконано комплекс палеомагнітних та магнітно-мінералогічних досліджень анортозитів і габро Володарськ-Волинського масиву Коростенського плутону з метою отримання нових палеомагнітних визначень, які задовольняють сучасні критерії надійності. Підтверджено, що у цих породах основним мінералом-носієм первинної залишкової намагніченості є магнетит та титаномагнетит з невеликою домішкою Ti. Біполярна характеристична компонента намагніченості, яка за усіма ознаками є первинною і має термозалишкову природу, виділяється у діапазоні температур 500–580 °C. Розрахований новий палеомагнітний полюс віком 1,76 млрд р. (Φ = 29,3°, Λ = 168,2°, A_{95} = 3,3°, N = 6) добре узгоджується із близькими за віком палеомагнітними визначеннями для габроїдів Інгульського та Волинського мегаблоків Українського щита, що свідчить про еволюцію цих мегаблоків в межах єдиної структури щита починаючи, щонайменше, з 1,76 млрд р. тому. Для уточнення часу амальгамації Східноєвропейської платформи, розрахунку її палеоширотного положення та кінематичних параметрів (швидкість широтного дрейфу, кутового обертання) її сегментів виконано вибірку найнадійніших палеомагнітних визначень для палеопротерозою Фенноскандії та Сарматії. Для окремих часових інтервалів виконано палеогеографічні реконструкції цих сегментів. Відповідно до палеомагнітних даних, їх остаточна амальгамація відбулася не раніше ніж 1,76 млрд р. тому, в цей час вони розташовувалися у екваторіальній області, Український щит (як частина Сарматії) був повернутий відносно Фенноскандії на ~40° проти годинникової стрілки.

Ключові слова: Коростенський плутон Український щит, габроїди, палеомагнетизм, петромагнетизм, палеомагнітний полюс, палеогеографічні реконструкції.

Received 29.09.2025